Int J Adv Manuf Technol (2010) 51:599–610
DOI 10.1007/s00170-010-2633-3

ORIGINAL ARTICLE

Determination of material removal rate in wire electro-discharge machining of metal matrix composites using dimensional analysis

Nilesh Ganpatrao Patil · P. K. Brahmankar

Received: 9 April 2009 / Accepted: 17 March 2010 / Published online: 16 April 2010

Abstract Wire electro-discharge machining (WEDM) is a vital process in manufacturing intricate shapes. The present work proposes a semi-empirical model for material removal rate in WEDM based on thermo-physical properties of the work piece and machining parameters such as pulse on-time and average gap voltage. The model is developed by using dimensional analysis and non-linear estimation technique such as quasi-Newton and simplex. Predictability of the proposed model is more than 99% for all work materials studied. The work materials were silicon carbide particulate reinforced aluminium matrix composites. The experiments and model prediction show significant role of coefficient of thermal expansion in WEDM of these materials. In addition, an empirical model, based on response surface method, has also been developed. The comparison of these models shows significant agreement in the predictions.

Keywords Wire electro-discharge machining · Dimensional analysis · Semi-empirical model · Metal matrix composites

1 Introduction

Wire electro-discharge machining (WEDM) is a widely accepted non-traditional material removal process used to manufacture components with intricate shapes and profiles. WEDM has been gaining wide acceptance in the machining of various materials used in modern tooling applications [1, 2]. Compared to die-sinking electrical discharge machining (EDM), WEDM is a technology with increasing economic importance in terms of units sold per year [3]. The settings for the various process parameters required in the WEDM process play crucial role in producing an optimal performance. The ultimate goal of the WEDM process is to achieve an accurate and efficient machining operation without compromise in the machining performance. This can mainly be achieved by understanding the inter-relationship between the large number of factors affecting the process and by identifying the optimal machining conditions.

Many attempts have been made to obtain the relationship between pulse conditions and material removal by solving time-dependent heat transfer equations assuming various heat source models [4–8]. Patel et al. [4] developed an anode erosion model considering Gaussian heat flux on the anode surface and shown that the plasma flushing efficiency is same for both cathode and anode. Erden and Kogmen [8] compared the performance characteristics and accuracy obtained from many of the earlier models. Recently, Yeo et al. [9] compared five EDM models from Snoeys, Van Dijck, Beck, Jilani and DiBitonto in terms of the temperature distribution, crater geometry and material removal at the cathode. Comparative analyses on the material removal rate (MRR) ratio of the predicted result to experimental data for discharge energy range from 0.33 to 952 mJ showed that DiBitonto's model yielded the closest proximity of 1.2–46.1 MRR ratio. They have suggested that the disk heat source models can be enhanced by improving the approximation of the heat flux and energy fraction. Table 1 shows the comparative study of these models and their accuracies in predicting MRRs. In addition to these thermal models of

N. G. Patil (✉) · P. K. Brahmankar
Department of Mechanical Engineering,
Dr. Babasaheb Ambedkar Technological University,
Lonere, Maharashtra 402103, India
e-mail: nileshgpatil@rediffmail.com

Table 1 Ratio of theoretical to experimental data (V=25 V, I=12.8 A, T_{on}=42 μs, material=AISI 4140) [9]

Model	Ratio of MRR
Snoey's model	1.9
Van Dijck's model	9.3
Beck's model	2.3
Jilani's model	2
Dibitonto's model	2.1

EDM, Singh and Ghosh [10] mentioned that for short pulse duration (<5 μs), the strong electric field at the cathode leads to mechanical stresses in the cathode material. These mechanical stresses were considered to contribute to material removal from the work piece in die-sinking EDM. However, in WEDM, the polarity of work piece is anodic, which may not be subjected to very high electric fields as in case of cathode. Thus, melting and/or evaporation have always been considered as the dominant material removal mechanism WEDM [11–13]. All of these and most of the many other theoretical models are concerned with die-sinking, in which cathodic workpiece polarity and rather long discharge times are employed. For WEDM, in which the work piece polarity is anodic and the pulses are of short duration with a highly transient discharge current, very few such models exist [11–13].

In addition, many different types of problem-solving quality tools have been used to investigate the significant factors and its inter-relationships with the other variables in obtaining an optimal WEDM performance [14–16]. In addition, the modelling of the WEDM process by means of empirical modelling techniques has also been applied to effectively relate the process parameters to the different performance measures of the WEDM process [17].

Literature shows that, basically, two separate approaches, the theoretical and the empirical, have been used in modelling of electro-discharge or WEDM process. The theoretical models show large discrepancy (Table 1) between the predictions and the experimental results due to simplified and unavoidable assumptions. On the other hand, the empirical models are limited to specific experimental conditions.

Moreover, it can be noted that there are very few attempts to model the WEDM process theoretically. Although, large number of efforts to empirically model this process has been made, to the best of the knowledge of the present authors, no model has been reported in WEDM of metal matrix composites (MMCs). Therefore, there exists a need to represent the process using the synergy of combination of theoretical and empirical methods. In view of this, the aim of this study was to develop a semi-empirical model in machining of ceramic reinforced aluminium matrix composites.

2 Machining of metal matrix composites

In recent years, the critical need for less expensive structural materials that can provide an optimum level of performance has generated considerable research interest in the development and application of MMCs. Clyne and Withers [18] discussed and suggested that use of MMC provides significant benefits including performance such as component's life and improved productivity. Kannan and Kishawy [19] mentioned that MMCs provide economic advantage through energy savings or lower maintenance cost and environmental benefits of lower noise levels and fewer air-borne emissions. Compared to the monolithic metals, MMCs have higher strength-to-weight ratios, better fatigue resistance, better elevated temperature properties, and lower coefficients of thermal expansion, improved thermal conductivity, good damping characteristics and excellent wear resistance. Further, it provides high flexibility in design. However, the utilisation of the MMC in different industries is not as generalised as expected due to difficulties in the machining of MMCs. Cost-effective machining has not yet been proven. Although primary fabrication processes such as casting, forging and extrusion have been well developed by a number of companies, cutting and finishing operations are still less well understood. Hung et al. [20] did extensive studies in machining of MMCs. They found that the ceramic particles that enhance the mechanical properties of MMCs and make them desirable also significantly reduce cutting tool life due to rapid abrasive wear. Chadwick and Heath [21] studied into machining of MMCs and shown that polycrystalline diamond (PCD) tools give longer service lives than carbide tools by 2–200 times and cause less sub-surface damage. Further, Heath [22] had shown that tool life of PCD tools is much longer as compared with cemented carbide tools. Davim [23] compared the performance of the diamond tools with chemical vapour deposition (CVD)-coated inserts and brazed PCD inserts in machining Al/SiC_p/20% composite. The life of PCD inserts was found to be almost ten times longer, with a cutting speed five times higher than that of CVD-coated tool. Further, the associated VB wear was about one third of that of CVD tool. Over the years, it has been found that the tool wear is rapid for cutting tools other than PCD. The literature review on conventional machining of MMCs reveals that only PCD is a suitable tool to machine these materials. However, it is too costly, and sub-surface damages, work hardening of matrix, delamination between matrix and particles and crack of particle or matrix are associated. Hence, poor machinability

makes it one of the most challenging types of materials to be processed especially when intricate parts and precision parts are required.

The non-conventional machining processes such as abrasive water jet machining and laser machining can be applied. However, the equipment is too expensive, and problems such as poor surface quality and limitation of work piece height are associated [24]. Recently, Liu et al. [25] studied on the mechanism of electrochemical discharge machining of Al/SiC composites. They have reported that the breakdown voltage in electrochemical discharge machining was much lower compared to conventional die-sinking EDM. In addition, the formation of Al_4C_3 phase was found on the EDM machined surfaces but not on the electrochemical discharge machined specimen. Thus, EDM has evolved as one of the promising choices to machine these materials.

Many researchers have worked in EDM of MMCs. Their findings include surface softening, effect of ceramic reinforcement on surface finish, effect of process parameters on surface finish and MRRs. The common conclusions of all these studies suggest that the ceramic particles do not melt and may only dislodge after melting of the surrounding matrix. Extensive studies have been made on die-sinking EDM of these materials. Comparatively, very few studies have been undertaken in WEDM of MMCs. Moreover, most of these studies have been done by using one-factor-at-a-time approach, which may not explain the effects of interaction among the various factors.

Some of the crucial findings are discussed here. Roux et al. [26] studied on the influence of EDM on surface integrity of Al/SiC/15% MMC. Their findings suggest negligible influence of the reinforcements on surface roughness. The surface roughness was found to be related to pulse energy alone. Extensive experimental study has been undertaken by Ramulu and Taya [27] on the EDM characteristics of Al/SiC_w composites. MRR was found to increase with increased power. The MRR and surface roughness were found to be higher for 15% reinforcement of SiCw. Hung et al. [28] reported, in EDM of Al/SiC_p, that only current dominates the surface finish, and the effect of voltage and on-time was negligible. In another study of the present authors on EDM of Al/SiC MMC, surface finish of MMC was found to be better than that of the unreinforced alloy, and MRR of MMC was lower than that of the unreinforced alloy [29]. In recent studies of the present authors on Al/Al_2O_{3p} composites, MRR was found to decrease with the increase in volume fraction of the alumina particles. However, surface finish was found to deteriorate with increased volume fraction of the ceramic reinforcements [30].

Yue and Dai [31] reported that surface finish of unreinforced matrix was superior than Al_2O_{3p} reinforced composites. Gatto and Iuliano [32] showed that the SiC reinforcement was absent in the recast layer after WEDM. Rozenek and Kozak [33] had shown that current and on-time influence the surface finish and cutting rate significantly in machining of alumina as well as silicon carbide reinforced aluminium matrix composites. Yan and Tsai [34], in an extensive one-factor-at-a-time experimental study on WEDM of Al/Al_2O_{3p} composites, concluded that the ceramic reinforcement was more significant than the energy level on surface finish of the MMCs. The surface roughness values were found to increase with increased volume fraction of the reinforcement. In WEDM of aluminium matrix composites, surface finish of MMCs was found to be significantly different than that of unreinforced alloy. However, the findings of various authors are also significantly different. These differences were due to the different range of parameters during the experiments, different matrix and different type and size of reinforcement particles.

Lau et al. [35] reported that MMCs can not be cut by WEDM process due to frequent wire breakage. In recent studies, Chiang and Chang et al. [36] have used grey relational method for multi-objective optimizations of Al_2O_{3p} reinforced composites. Dhar et al. [37] have developed non-linear empirical model using design of experiments in EDM of Al/SiC composites. The analysis of variance was performed to verify the fit and adequacy of the developed models. Karthikeyan et al. [38] employed full factorial design of experiments to model MRR and TWR in EDM of Al/SiC composites empirically. The present authors have recently reported their findings on the effects of volume fraction of SiC particulates in WEDM of MMCs [39]. The recent experimental study by Cichosz and Karloszak [40] on die-sinking EDM of Al/Al_2O_{3f} MMCs reported formation of Al–O compound on the machined surfaces. They have reported the correlation between the formation of recast layer and discharge current.

It is thus observed that published work on the EDM characteristics of MMCs is reasonably extensive. However, the understandings into WEDM of MMCs have not been optimised. The issues such as wire breakage and poor surface quality are still not completely understood while machining these materials. Further, the works done so far have not been incorporated into any modelling and optimization activity. Therefore, the present work is an attempt in that direction. In this study, two different models of MRR have been developed. The first model is an empirical model developed by using statistical approach. The response surface methodology (RSM) was employed to develop this model. In another attempt, a semi-empirical model has been developed. The following sections deal with the development of these models, and finally, a comparison of these models is presented.

3 Development of response surface model

RSM approach is the procedure for determining the relationship between various process parameters with the various machining criteria and exploring the effect of these process parameters on the responses. RSM is a dynamic and foremost important tool of design of experiment wherein the relationship between response(s) of a process with its input decision variables is mapped.

In order to study the effect of WEDM process parameters of MMCs on the MRR, a second-order polynomial response can be fitted. In RSM, the quantitative form of relationship between the desired response and the independent input variables [41] could be represented as:

$$Y_i = f(X_1, X_2, X_3, X_4) \pm \varepsilon \tag{1}$$

where, x_1, x_2, x_3 and x_4 are the coded values of the variables pulse on-time, off-time, average voltage and ceramic volume fraction, respectively. A_m, B_m, U_m and V_{fm} are the values of pulse on-time, off-time, average voltage and ceramic volume fraction at zero level, respectively.

The coded numbers of the input parameters in Eq. 1 are obtained from the following transformation:

$$\text{Pulse on} - \text{time}, X_1 = \frac{A - A_m}{\Delta A} \tag{2}$$

$$\text{Pulse off} - \text{time}, X_2 = \frac{B - B_m}{\Delta B} \tag{3}$$

$$\text{Average gap voltage}, X_3 = \frac{U - U_m}{\Delta U} \tag{4}$$

$$\text{Volume fraction}, X_4 = \frac{V_f - V_{fm}}{\Delta V_f} \tag{5}$$

In the present study, experiments were designed on the basis of experimental design technique proposed by Box and Hunter [42]. The uniform-precision rotatable central composite, face centre design, experimental design (CCD), as demonstrated by Myers and Montgomery [43], was used to improve the reliability of the results and to reduce the size of experiments without loss of accuracy. This design consists of 16 factorial, two replicate (coded level ±1) runs, eight axial runs as well as six central trials. The strategy of complete randomization was adopted for conducting the experiments. Based on the extensive preliminary investigations, literature and the experience of machine operators, input parameters (control factors) were selected to develop empirical models for WEDM in machining of Al/SiC_p composites. Pulse on-time (microsecond), pulse off-time (microsecond), average voltage (volt) and volume fraction of ceramic reinforcements (percent) were selected as the input parameters. Table 2 shows the levels and range of these parameters for the experiments as well as their codes. The experimental matrix employed in this study is shown in Table 3.

The appearance of response function is a surface as plotting the expected response of **f**. The identification of suitable approximation of **f** will determine whether the application of RSM is successful or not. In this study, the approximation of **f** will be proposed using the fitted second-order polynomial regression model, which is called the quadratic model. The quadratic models of y_i for four input parameters can be written as follows:

$$Y_{\text{MRR}} = \alpha_0 + \sum_{i=1}^{4} \alpha_i x_i + \sum_{i=1}^{4} \alpha_{ii} x_i^2 + \sum_{j>i}^{4} \alpha_{ij} x_i x_j \tag{6}$$

where α_0 is constant for MRR, and α_i represents the coefficients of linear terms. The quadratic and interaction terms are denoted by α_{ii} and α_{ij}, respectively. Here, x_i is the variable corresponding to process parameters such as on-time, off-time, average voltage and ceramic volume fraction. The response surface may contain linear terms, squared terms and interaction terms. The proposed quadratic model of Y_i in this study investigates over the entire process parameter space. The necessary data for building the response model was collected by the design of experiments. These experimental results are shown in the CCD design matrix (Table 3).

Table 2 Experimental parameters settings (central composite)

Level	Pulse on-time, A (μs)	Pulse off-time, B (μs)	Average voltage, U (V)	Volume fraction, V_f (%)
−2	0.4	12	40	10
−1	0.4	12	40	10
0	0.7	14	45	20
+1	1	16	50	30
+2	1	16	50	30

Table 3 Results of the statistically designed experiments

Std. No.	A	B	U	V_f	MRR, mm^2/min
1	0.4	12	40	10	48
2	1	12	40	10	118
3	0.4	16	40	10	36
4	1	16	40	10	98
5	0.4	12	50	10	36
6	1	12	50	10	100
7	0.4	16	50	10	26
8	1	16	50	10	78
9	0.4	12	40	10	48
10	1	12	40	10	116
11	0.4	16	40	10	36
12	1	16	40	10	98
13	0.4	12	50	10	36
14	1	12	50	10	100
15	0.4	16	50	10	26
16	1	16	50	10	78
17	0.4	12	40	30	38
18	1	12	40	30	90
19	0.4	16	40	30	28
20	1	16	40	30	72
21	0.4	12	50	30	26
22	1	12	50	30	72
23	0.4	16	50	30	20
24	1	16	50	30	56
25	0.4	12	40	30	38
26	1	12	40	30	90
27	0.4	16	40	30	28
28	1	16	40	30	74
29	0.4	12	50	30	28
30	1	12	50	30	74
31	0.4	16	50	30	20
32	1	16	50	30	56
33	0.4	14	45	20	28
34	1	14	45	20	78
35	0.7	12	45	20	56
36	0.7	16	45	20	42
37	0.7	14	40	20	56
38	0.7	14	50	20	42
39	0.7	14	45	10	62
40	0.7	14	45	30	47
41	0.7	14	45	20	49
42	0.7	14	45	20	50
43	0.7	14	45	20	50
44	0.7	14	45	20	50
45	0.7	14	45	20	51
46	0.7	14	45	20	50

The constants and coefficients for the model were determined by using the experimental results. The final form of the model is shown below:

$$\begin{aligned}\mathrm{MRR} = {} & 75.2343 + (153.55 \times A) - (1.68382 \times B) - (0.525 \times U) \\ & - (2.55906 \times V_f) + (44.2603 \times A^2) + \left(0.0548343 \times V_f^2\right) \\ & - (3.75 \times AB) - (1.25 \times AU) - (1.41667 \times AV_f) + (0.0375BV_f)\end{aligned} \tag{7}$$

The adequacy of the proposed models was also checked by the variance analysis (F test). The R value for the MRR model is 0.99. It indicates very good fit and agreement between experiments and the model predictions. Table 4 shows the analysis of variance of the presented response surface regression equation. In the next section, development of semi-empirical model using dimensional analysis and non-linear estimation is presented. Comparisons between the predictions of these empirical and semi-empirical models are made in the following section.

4 Development of dimensional analysis model

It has been demonstrated that the MRR can be predicted using empirical models such as response surface models. However, these models are limited to the machining settings parameters and they do not consider the effects of work material properties on the process performance. Therefore, it was decided to develop a model which includes the machining parameters as well as material-specific parameters.

The present work uses the technique of dimensional analysis to develop a semi-empirical model of MRR in WEDM of Al/SiC composites. Dimensional analysis is a method by which we deduce information about a phenomenon from the single premise that the phenomenon can be described by a dimensionally correct equation among certain variables. The theory of dimensional analysis is the mathematical theory which is purely algebraic. The application of dimensional analysis to a practical problem is based on the hypothesis that the solution of the problem is expressible by means of a dimensionally homogeneous equation in terms of specified variables [44].

Table 4 Analysis of variance

Source	DF	SS	MS	F	P
Regression	10	31,251.6	3,125.16	3,000	0.000
Residual error	35	35.9	1.03		
Lack-of-fit	14	25.9	1.85	3.89	0.03
Pure error	21	10	0.48		
Total	45	31,287.5			

In WEDM of MMCs, the material removal is by melting and/or evaporation of the electrically conductive phase, i.e. aluminium in the present case. A possible mechanism for formation of craters is that sparks are formed at the conductive phase. Similar findings were reported by Gadalla in electric discharge machining of WC-Co [45, 46]. In addition, it has also been observed and reported by many other researchers [24, 29, 30, 34]. The same mechanism might be possible due to low melting temperature and high electrical conductivity of the aluminium alloy as compared to the ceramic (SiC_p) reinforcements. This "selective sparking" between aluminium alloy and the cathode wire might be attributed to the high electric resistance of the ceramic (SiC) reinforcements. Thus, the spark might, obviously, follow the path of least resistance and jump on the conductive aluminium alloy matrix. This electrical energy in the form of spark energy transferred into heat energy. Maximum part of this heat energy is delivered to the anodic work piece in the first few microseconds. Therefore, in WEDM, even at small on times, the temperature of anode is raised beyond boiling point temperature of the matrix alloy. During off-time, the insulating phase (SiC_p) is dislodged, and the resulting cavities are partially smeared by the liquid phase. The residual cavities depend on the amount of molten metal. Thus, the part of heat conducted into the work piece and the amount of molten material was found to be influenced by the thermal properties of the work material. The amount of electrical energy, i.e. spark energy and intensity of discharge power, might be influenced by the electrical properties of the electrodes. Besides, the supplied energy in the spark gap is determined by the pulse parameters such as on-time, peak discharge current and voltage.

Thus, based on the literature, it can be said that no single material property of the work or tool material can predict its eroded volume. The electrical, thermal properties along with the pulse condition might determine the performance of the WEDM process. The thermal, physical properties of the material as well as the pulse on-time and average gap voltage are found to be the most significant parameters for MRR [39, 47].

In the developed model, the thermo-physical properties of the machined materials like thermal conductivity, electrical conductivity, density, specific heat, melting temperature, thermal coefficient of expansion and latent heat of fusion were considered. The machining process parameters such as pulse on-time and average gap voltage were also considered along with these material properties. The dimensions of these variables as well as their values for the machined materials are shown in Table 5.

Applying dimensional analysis, the MRR, V can be given by an equation of the form,

$$V = f\left(T_{\text{on}},\ U,\ \rho,\ K,\ \sigma,\ C_p,\ T_m,\ \varepsilon,\ L_f\right) \tag{8}$$

where, T_{on} is the pulse on-time, and U is the average gap voltage. The units of on-time and gap voltage are microsecond and voltage, respectively. Further, the dimensions for on-time and gap voltage are T and $ML^2T^{-3}I^{-1}$, respectively.

4.1 Buckingham's π theorem

In the present study, this theorem is used to assemble all variables appearing in the problem in a number of dimensionless products (π_s). The required relations connecting the individual variables are determined as algebraic expressions relating π_s.

A dimensional matrix is then formulated as shown in Table 6, where the dependent as well as independent variables are defined as per their fundamental dimensions [44], where x_1, x_2, x_3, x_4, x_5, x_6, x_7, x_8, x_9 and x_{10} are the indices of the variables in Eq. 8, respectively.

It is necessary to choose the repeating and non-repeating variables to develop a model using the Π-theorem. The

Table 5 Units, dimensions and thermo-physical properties of the machined materials

Properties	Symbol	Dimensions	Work piece material		
			Al/SiC_p/10%	Al/SiC_p/20%	Al/SiC_p/30%
Density, kg/m^3	P	ML^{-3}	2,710	2,765	2,798
Thermal conductivity, W/m-K	K	$MLT^{-3}\theta^{-1}$	156	150	144.5
Electrical conductivity, Siemens/m	Σ	$M^{-1}L^{-3}T^3I^2$	19.83×10^6	15.3×10^6	11.136×10^6
Specific heat, J/kg-K	C_p	$L^2T^{-2}\theta^{-1}$	879	837	795
Melting point, K	T_m	θ	828	828	828
Thermal coefficient of expansion, K^{-1}	E	θ^{-1}	20.7	17.46	14.58
Heat of fusion, J/kg	L_f	L^2T^{-2}	389×10^3	389×10^3	389×10^3

M mass, L length, T time, θ temperature, I current

Table 6 Model parameters in the form of their fundamental dimensions

Dimensions	Model parameters									
	x_1 V	x_2 T_{on}	x_3 U	x_4 T_m	x_5 L_f	x_6 σ	x_7 C_p	x_8 K	x_9 ρ	x_{10} ε
M (mass)	0	0	1	0	0	−1	0	1	1	0
L (length)	3	0	2	0	2	−3	2	1	−3	0
T (time)	−1	1	−3	0	−2	3	−2	−3	0	0
θ (temperature)	0	0	0	1	0	0	−1	−1	0	−1
I (current)	0	0	−1	0	0	2	0	0	0	0

number of repeating variables is equal to the number of fundamental dimensions. Thus, five variables were selected as repeating variables on the basis of the following conditions:

1. The dependent variable (MRR) should not be the repeating variable.
2. The repeating variables should be of different properties.
3. Repeating variables should not form a dimensionless group.
4. Repeating variable together should have the same number of fundamental dimensions (five in the present case).
5. No two repeating variables should have the same dimensions.

Thus, machining setting parameters (on-time and average voltage) along with melting temperature and heat of fusion were selected as the non-repeating parameters. The dependent variable, MRR, was also selected as non-repeating variable. Other properties of work materials were thus chosen as the repeating parameters.

If an equation is dimensionally homogeneous, it can be reduced to a relation with a complete set of dimensionless products. Therefore, if n variables are connected by dimensionally homogeneous equation, the equation can be expressed in the form of a relation between n–r dimensionless products π_s, where n–r is the number of products in a complete set, where n is the number of variables and r is the rank of matrix shown in Table 6. In most cases, r is equal to the number of fundamental dimensions in the problem. In the present case, the fundamental dimensions are mass (M), length (L), time (T), temperature (θ) and current (I). Therefore, since the total variables are ten and the fundamental dimensions are five,

n=10 and r=5,

hence,

$$n-r=5 \text{ in the present study}$$

Therefore,

$$f(\Pi_1, \Pi_2, \Pi_3, \Pi_4, \Pi_5)=0 \tag{9}$$

Now, the dimensional formula for the relation in Eq. 8 can be written as

$$[L^3T^{-1}]^{X1}[T]^{X2}[ML^2T^{-3}I^{-1}]^{X3}[\theta]^{X4}[L^2T^{-2}]^{X5}[M^{-1}L^{-3}T^3I^2]^{X6} \left[L^2T^{-2}\theta^{-1}\right]^{X7}\left[MLT^{-3}\theta^{-1}\right]^{X8}[ML^{-3}]^{X9}\left[\theta^{-1}\right]^{X10}=[M^0L^0T^0\theta^0I^0]. \tag{10}$$

By equating the powers of the fundamental units on both sides of Eq. 10, a set of simultaneous equations are obtained. These equations are later solved to obtain the magnitudes of these constants. The five dimensionless products are then determined by solving for the x_s. The results of dimensional analysis are shown in Table 7. The detailed derivation of this model is given in the Appendix.

Hence, as per the results shown in Table 7, the following complete set of dimensionless products is obtained:

$$\prod_1 = V\sqrt{\frac{C_p}{\alpha^4\varepsilon}}$$

$$\alpha=\frac{K}{\rho C_p}$$

Table 7 Results of dimensional analysis

	Π_1	Π_2	Π_3	Π_4	Π_5
x_1	1	0	0	0	0
x_2	0	1	0	0	0
x_3	0	0	1	0	0
x_4	0	0	0	1	0
x_5	0	0	0	0	1
x_6	0	0	1/2	0	0
x_7	2.5	2	0	0	−1
x_8	−2	−1	−1/2	0	0
x_9	2	1	0	0	0
x_{10}	−1/2	−1	1/2	1	1

where α=thermal diffusivity, m^2/s,

$$\prod_2 = \frac{T_{on} C_p}{\alpha\varepsilon}$$

$$\prod_3 = U\sqrt{\frac{\sigma\varepsilon}{K}}$$

$$\prod_4 = T_m\varepsilon$$

$$\prod_5 = \frac{L_f\varepsilon}{C_p}$$

Note that Eq. 9 can also be written as

$$\Pi_1 = f(\Pi_2, \Pi_3, \Pi_4, \Pi_5) \tag{11}$$

Therefore, the final form of the model can be written as below:

$$V = A\sqrt{\frac{\alpha^4\varepsilon}{C_p}}\left(\frac{C_p T_{on}}{\alpha\varepsilon}\right)^a \left(\frac{U^2\sigma\varepsilon}{K}\right)^b (T_m\varepsilon)^c \left(\frac{L_f\varepsilon}{C_p}\right)^d \tag{12}$$

where, A is the coefficient, and a, b, c and d are the power indexes of the corresponding dimensionless bracket, i.e. Π_s.

The most noticeable aspect in this model is the appearance of thermal coefficient of expansion (ε) in all the dimensional products. It suggests the significance of this property in WEDM process.

The semi-empirical model of the MRR shown as Eq. 12 includes both the machining process parameters as well as the thermo-physical properties of the work material. The coefficients (A) and the power indices (a, b, c and d) in Eq. 12 need to be calculated. Therefore, a set of experiments has been conducted, and based on these experimental results, the coefficients and power indices of Eq. 12 have been determined by using non-linear estimation.

In the most general terms, non-linear estimation computes the relationship between a set of independent variables and a dependent variable. Estimation is the process of fitting a mathematical model to experimental data to determine unknown parameters in the model. The parameters are chosen so that the output of the model is the best match to the experimental data. The estimation process is often non-linear because the observed data do not vary in direct proportion to the parameters in question.

In the present case, non-linear estimation methods, namely, the simplex and quasi-Newton, were employed to determine the model parameters.

The experiments were performed by using Charmilles technology WEDM machine tool (Robofill 290). Plain brass wire (CuZn37) was employed as the electrode. The diameter of wire was 0.25 mm. Deionised water was used as the dielectric. The electrical conductivity of the dielectric was maintained at 15 μS/cm. The temperature of dielectric was maintained at 22°C. Table 8 shows the machining parameter settings used for the experiments.

Table 8 Fixed machining parameters

Fixed parameters	Fixed level
Workpiece height	20 mm
Length of cut	20 mm
Angle of cut	Vertical
Location of the workpiece on the table	Centre of the table
Temporary reduction in frequency (FF)	100
Tac	0.4 μs
Pulse off-time	12 μs
Wire speed	10 m/min
Wire tension	10 N
Pulse on-time	0.2, 0.4, 0.6, 0.8 and 1.0 μs
Average gap voltage	40, 45, 50 V
Work material[a]	Al/SiC_p/10%, 20% and 30%
Wire electrode	Brass wire, 0.25 mm diameter, CuZn37
Dielectric	Deionised water, 15 μS/cm

[a] Duralcan MMCs

The adequacy of these models is checked by the correlation coefficient R, the mean error ME, the root mean square error RMSE and the average percentage error, ΔE_{av}%. For this analysis of correlation, the following equations were used:

$$\text{ME} = \frac{1}{n}\sum_{i=1}^{n}(Y_i - Y) \tag{13}$$

$$\text{RMSE} = \sqrt{\frac{1}{n}\sum_{i=1}^{n}(Y_i - Y)^2} \tag{14}$$

$$\Delta E_{av}\% = \frac{1}{n}\sum_{i=1}^{n}\frac{Y_i - Y}{Y_i} \times 100 \tag{15}$$

where, Y_i is the ith result from the model, and Y is the corresponding experimental result. The coefficients and power indices determined by using non-linear estimation are shown in Table 9.

5 Discussion

Figure 1 shows the topography of the machined surfaces. It shows the evidence of the melting of the work piece material due to WEDM. The recast layer is the layer of re-solidified aluminium alloy which was melted under the action of WEDM. The surface morphology also shows liquid-like formation on the machined surfaces.

Table 9 The coefficients and indexes of the material removal rate model

	Al/SiC$_p$/10%	Al/SiC$_p$/20%	Al/SiC$_p$/30%
A	2.254	2.086	1.966
A	1.1775	1.1535	1.1154
B	−2.3403	−1.959	−2.266
C	−0.237	−0.8673	−1.1
D	0.1514	0.5688	1.05
R	0.999	0.996	0.995
ME	−0.06	0.043	−0.15
RSME	1.2	2.3	2.01
ΔE_{av}%	0.04	0.001	0.021

Results of experiments and predictions of two models, empirical and semi-empirical, are shown in Figs. 2, 3, 4 and 5.

These results show that the MRR of Al/SiC$_p$/10% composites is much better as compared to the 20% and 30% ceramic reinforced composites. This may be attributed to lower thermal coefficient of expansion, low thermal conductivity, lower thermal diffusivity and lower electrical conductivity of the 20% and 30% SiC reinforced MMCs. Besides, the high percentage of ceramic reinforcement not only changes the thermo-physical properties of the material but also affects the machining performance by alterations caused in the gap status.

The results indicate that the model is dependent on the materials of the work piece and therefore cannot be represented by a set of universal coefficients and power indexes for all the materials studied. The model indicates that coefficient of thermal expansion is the most important property in WEDM since it appears in all the brackets of the model. In addition, thermal diffusivity and T_{on} seem to be the significant variables.

The energy that is delivered to the workpiece by the plasma channel can be divided into two parts. One is used to heat up the workpiece, while the other part is conducted into the workpiece. Thus, the amount of heating and volume of molten material is determined by the thermal diffusivity and the melting temperature of the workpiece material. The thermal diffusivity is further determined by the thermal conductivity, specific heat and density. The total molten metal, however, does not flush away, and some parts of this molten volume remain on the workpiece

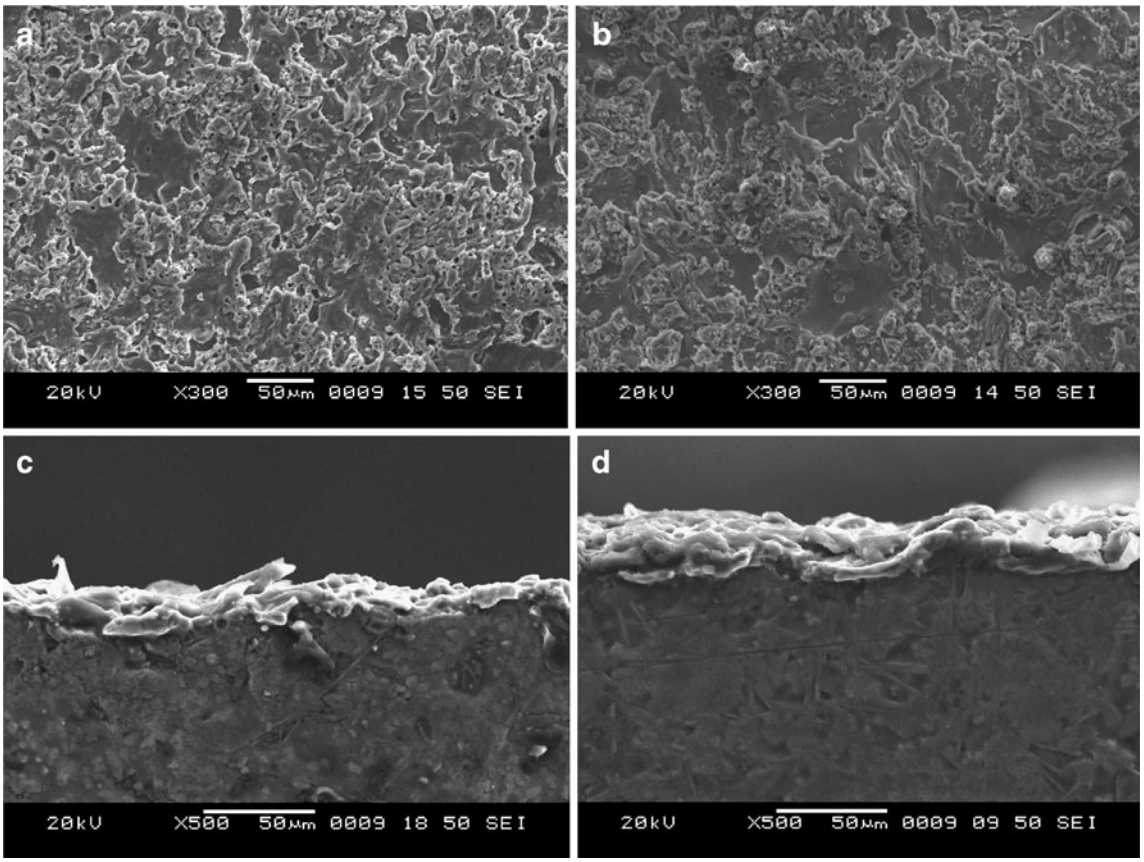

Fig. 1 Machined surface of (**a**) Al/SiC$_p$/20% composite and (**b**) Al/SiC$_p$/30% and recast layer of (**c**) Al/SiC$_p$/20% composite and (**d**) Al/SiC$_p$/30% metal matrix composite

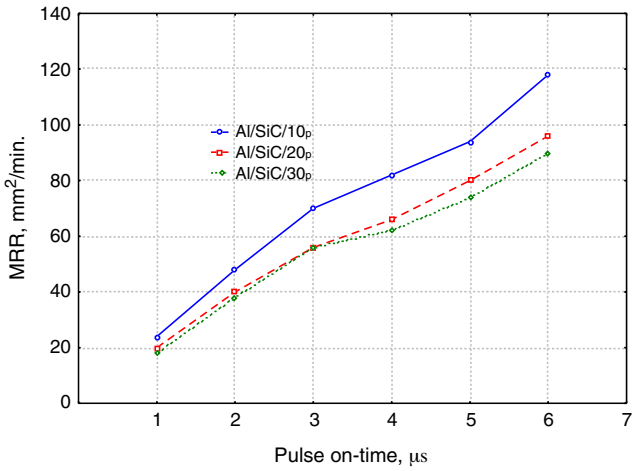

Fig. 2 Comparison of material removal rate in Al/SiC_p composites

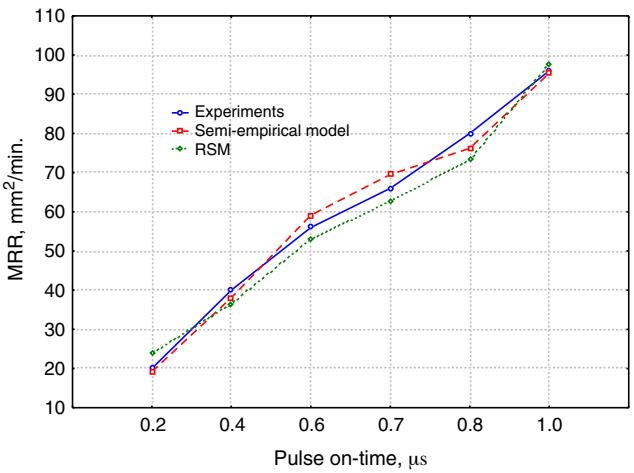

Fig. 4 Verification of predicted values in Al/SiC_p/20% composite

surface as a recast layer (Fig. 1). The ejection of molten material at the end of the on-time removes significant amount of molten metal and also determines the fraction of total molten material effectively removed from the workpiece. The efficiency of ejection of this molten material from the surface was found to depend on the thermal coefficient of expansion, the amount of molten material, discharge channel radius, thermal properties of the material and the flushing conditions [48]. The present model agrees with these findings, where the coefficient of thermal expansion was found to be the most influential material property along with thermal diffusivity on the MRR. In addition, the on-time which determines the discharge energy as well as the discharge channel radius was also found to influence the MRR. However, in the present case, the volume fraction of the ceramic reinforcements was also found to affect the MRR significantly. Although, the effect of ceramic reinforcements was taken into account while determining the properties of these materials, additional effect of ceramic reinforcements in terms of gap contamination, change in fluidity of the molten material and the ejection efficiency of the molten metal might also be significant.

Comparisons of the predicted results using the RSM model and the semi-empirical model are presented in Figs. 2, 3, 4 and 5. Results show good agreement between the two different models and the experiments. However, a significant difference exists between MRR predicted by the RSM and the semi-empirical model at 0.2 μs on-time. The RSM model predicts higher MRR as compared to the semi-empirical model and the experimental results. This difference might be attributed to the role of dislodged SiC particles in the spark gap. These particles may alter the gap status. At lower on-time, the energy in the gap is not enough, and the presence

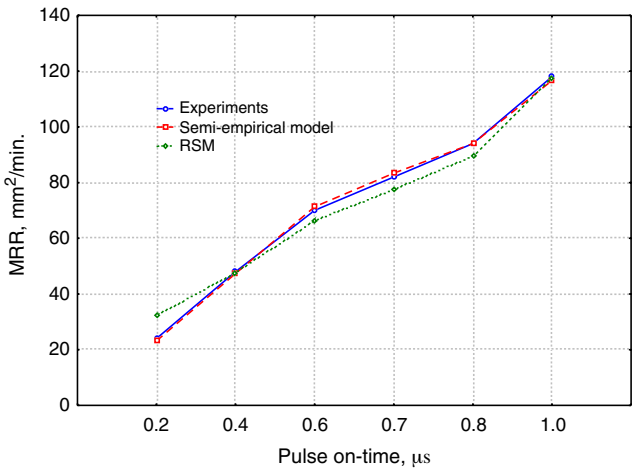

Fig. 3 Verification of predicted values in Al/SiC_p/10% composite

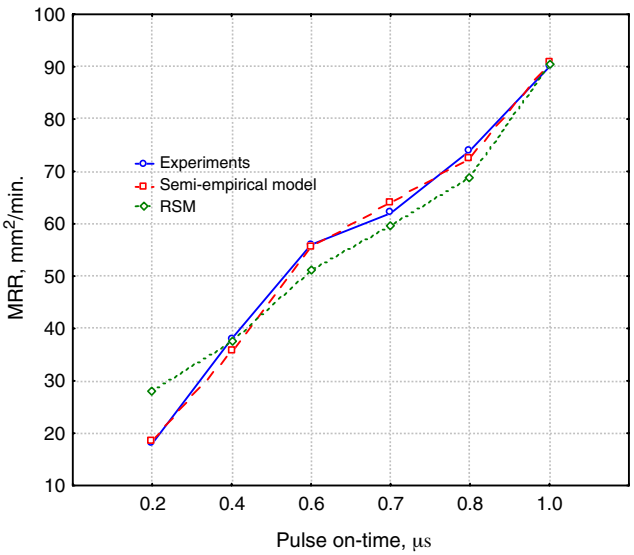

Fig. 5 Verification of predicted values in Al/SiC_p/30% composite

of insulating SiC particles in the gap reduces the MRR significantly. Therefore, at low spark energy, the RSM model could not predict as accurately as the semi-empirical model. In addition, the range of parameters selected for the RSM experiments was between 0.4 and 1 μs on-time.

Compared to all the empirical models proposed earlier, the semi-empirical model is mainly based on the thermal, physical and electrical properties of the work along with the machining process parameters on-time and average voltage. Although this model is not universal, the teamwork of dimensional analysis and statistical methods makes this methodology a very good option to look into further issues of the process in more details. This methodology can be further employed for investigating the surface quality of the machined surfaces as well as for wire tool performance.

6 Conclusions

A different approach, combination of dimensional analysis and non-linear estimation methods, is used in the modelling of WEDM of difficult-to-cut MMCs. Finally, the following conclusions can be drawn:

- The predictability of the RSM and the semi-empirical model is more than 99%.
- Predictions of the empirical as well as empirical models agree significantly with the experiments. However, the agreement was found to be limited at low level of pulse on-time (0.2 μs).
- The coefficients and power indices of the model suggests that pulse on-time and thermo-physical properties such as coefficient of thermal expansion, thermal diffusivity and melting point temperature are significant parameters on MRR.
- The experimental results show that increased percentage of ceramic particulates in the MMC causes decreased MRR. The decrease in MRR is almost 12% with an increase of 10% in ceramic reinforcements.
- Although the present models may not be suitable for different machining conditions, the methodology can be employed in the process to study the process in further details.
- It could be used to unveil the issues such as wire performance, gap status and surface integrity of the machined components.

Acknowledgements The authors are thankful to Duralcan, USA, for providing the MMC materials. Thanks are due to Mr. H.D. Kapse, Mr. R.D. Patil and Mr. Nere of Indo-German Tool Room, Aurangabad, India, for the WEDM facility. The authors would like to acknowledge the help from Prof. Pathak, Prof. Peshwe, Ms. Gauri Deshmukh and Prof. C.L. Gogte of VNIT, Nagpur, India, for SEM investigations.

Appendix

The set of simultaneous equation:

$$\begin{aligned} &x_3 - x_6 + x_8 + x_9 = 0 \\ &3x_1 + 2x_3 + 2x_5 - 3x_6 + 2x_7 + x_8 - 3x_9 = 0 \\ &-x_1 + x_2 - 3x_3 - 2x_5 + 3x_6 - 2x_7 - 3x_8 = 0 \\ &x_4 - x_7 - x_8 - x_{10} = 0 \\ &-x_3 + 2x_6 = 0 \end{aligned} \tag{16}$$

This simultaneous equation can be written in the matrix form:$\mathbf{AX}=C_1$

$$\mathbf{A} = \begin{vmatrix} -1 & 0 & 1 & 1 & 0 \\ -3 & 2 & 1 & -3 & 0 \\ 3 & -2 & -3 & 0 & 0 \\ 0 & -1 & -1 & 0 & -1 \\ 2 & 0 & 0 & 0 & 0 \end{vmatrix} \quad \mathbf{X} = \begin{vmatrix} X_6 \\ X_7 \\ X_8 \\ X_9 \\ X_{10} \end{vmatrix} \tag{17}$$

Then, assigning $x_1=1$ and x_2 to $x_5=0$ gives the following equation:

$$\begin{aligned} C &= [0 \quad -3 \quad 1 \quad 0 \quad 0]^T \\ X &= [0 \quad 2.5 \quad -2 \quad 2 \quad -0.5]^T \end{aligned} \tag{18}$$

Therefore,

$$\prod_1 = V\sqrt{\frac{C_p}{\alpha^4 \varepsilon}} \tag{19}$$

where,

$$\alpha = \frac{K}{\rho C_p} \tag{20}$$

Then, using the procedure further, $x2=1$, $x3=\ldots$ were assigned to determine π_2, π_3, π_4 and π_5.

References

1. Ho KH, Newman ST (2004) State of the art in wire electrical discharge machining (WEDM). Int J Mach Tools Manuf 44:1247–1259
2. McGeough JA (1988) Electrodischarge machining. Advanced methods of machining. Chapman & Hall, London, p 130
3. Altpeter F, Perez R (2004) Relevant topics in wire electrical discharge control. J Mater Process Technol 149:147–151
4. Patel MR, Barrufet MA, Eubank PhT, Dibitonto DD (1989) Theoretical models of the electrical discharge machining process-II: the anode erosion model. J Appl Physi 66(9):4104–4111
5. Erden A, Kaftanoglou B (1981) Heat transfer modelling of electric discharge machining. Proceedings of the 21st International Machine Tool Design and Research Conference, Swansea, pp 351–358
6. Snoeys R, Van Dijck WL (1972) Plasma channel diameter growth affects stock removal in EDM. CIRP Ann 21(1):39–40
7. Jilani ST, Pandey PC (1982) Analysis and modelling of EDM parameters. Precis Eng 4(4):215–221
8. Erden A, Kogmen M (1995) Comparison of mathematical models for electric discharge machining. J Mater Process Manuf Sci 4:163–176
9. Yeo SH, Kurnia W, Tan PC (2008) Critical assessment and numerical comparison of electro-thermal modes in EDM. J Mater Process Technol 203:241–251

10. Singh A, Ghosh A (1999) A thermo-electric model of material removal during electric discharge machining. Int J Mach Tools Manuf 39:669–682
11. Spur G, Schonbeck J (1993) Anode erosion in wire-EDM-A theoretical model. CIRP Ann 42(1):253–256
12. Han F, Jiang J, Yu D (2007) Influence of discharge current on machined surfaces by thermo-analysis in finish cut WEDM. Int J Mach Tools Manuf 47(7–8):1187–1196
13. Han F, Jiang J, Yu D (2007) Influence of machining parameters on surface roughness in finish cut of WEDM. Int J Adv Manuf Technol 34:538–546
14. Scot D, Rajurkar KP (1991) Analysis and optimization of parameter combinations in wire electrical discharge machining. Int J Prod Res 29(11):2189–2207
15. Tarng YS (1995) Determination of Optimal cutting parameters in wire electrical discharge machining. Int J Mach Tools Manuf 135 (12):1693–1701
16. Liao YS, Huang JT, Su HC (1997) A study on machining-parameters optimization of wire electrical discharge machining. J Mater Process Technol 71:487–493
17. Spedding TA, Wang ZQ (1997) Study on modelling of wire EDM process. J Mater Process Technol 69:18–28
18. Clyne TW, Whithers PJ (1992) An introduction to metal matrix composites. Cambridge University Press, London
19. Kannan S, Kishawy HA (2006) Surface characteristics of machined aluminium metal matrix composites. Int J Mach Tools Manuf 46(15):2017–2025
20. Hung NP, Loh NN, Venkatesh VC (1999) Machining of metal matrix composites. Machining of ceramics and composites. Marcel Dekker, Inc, New York, pp 295–298
21. Chadwick GA, Heath PJ (1990) Machining metal matrix composites. Metal Mater 6:73–76
22. Heath PJ (2001) Developments in applications of PCD tooling. J Mater Process Technol 116:31–38
23. Davim JP (2002) Diamond tool performance in machining metal matrix composites. J Mater Process Technol 128:100–105
24. Muller F, Monaghan J (2000) Non-conventional machining of particle reinforced metal matrix composite. Int J Mach Tools Manuf 40:1351–1366
25. Liu JW, Yue TM, Guo ZM (2009) An analysis of the discharge mechanism in electrochemical discharge machining of particulate reinforced metal matrix composites. Int J Mach Tools Manuf. doi:10.1016/j.ijmachtools.2009.09.004
26. Roux TL, Wise LH, Aspinwall DK (1993) The effect of electrical discharge machining on the surface integrity of an aluminium-silicon carbide metal matrix composite. J Process Adv Mater 3:233–241
27. Ramulu M, Taya M (1989) EDM machinability of SiCw/Al composites. J Mater Sci 24:1103–1108
28. Hung NP, Yang LJ, Leong KW (1994) Electrical discharge machining of cast metal matrix composites. J Mater Process Technol 44:229–236
29. Patil NG, Brahmankar PK (2006) Some investigations into wire electro-discharge machining performance of Al/SiCp composites. Int J Mach Mach Mater 1(4):412–431
30. Patil NG, Brahmankar PK (2009) Some studies into wire electro-discharge machining of alumina-particulate reinforced aluminium matrix composites. Int J Adv Manuf Technol. doi:10.1007/s00170-009-2291-5
31. Yue TM, Dai Y (1996) Wire electrical discharge machining of Al_2O_3 particle and short fiber reinforced aluminum based composites. Mater Sci Technol 12:831–835
32. Gatto A, Iuliano L (1997) Cutting mechanisms and surface features of wed machined metal matrix composites. J Mater Process Technol 65:209–214
33. Rozenek M, Kozak J (2001) Electric discharge characteristics of metal matrix composites. J Mater Process Technol 109:367–370
34. Yan BH, Tsai HC (2005) Examination of wire electrical discharge machining of Al_2O_{3p}/6061Al composites. Int J Mach Tools Manuf 45(3):251–259
35. Lau WS, Yue TM, Lee TC, Lee WB (1995) Un-conventional machining of composite materials. J Mater Process Technol 48:199–205
36. Chiang Ko-Ta, Chang Fu-Ping (2006) Optimization of the wedm process of particle-reinforced material with multiple performance characteristics using grey relational analysis. J Mater Process Technol 180:96–101
37. Dhar S, Purohit R, Saini N, Sharma A, Hemanth kumar G (2007) Mathematical modelling of electric discharge machining of cast Al-4Cu-6Si alloy- 10 wt.% SiC_p composites. J Mater Process Technol 194:24–29
38. Karthikeyan R, Lakshmi Narayan PR, Naagarazan RS (1999) Mathematical modelling for electric discharge machining of aluminium-silicon carbide particulate composites. J Mater Process Technol 87:59–63
39. Patil NG, Brahmankar PK (2009) Some investigations into combined effect of ceramic reinforcement and process parameters into electro-discharge machining of Al/SiC_p composites. J Form Mach Technol 1:113–128
40. Cichosz P, Karloszak P (2008) Sinker electrical discharge machining of aluminium matrix composites. Mater Sci (Poland) 26(3):547–554
41. Montgomery DC (2001) Design and analysis of experiments. Wiley, New York
42. Box GE, Hunter JS (1957) Multifactor experimental designs. Ann Math Stat 28:195–241
43. Myers RH, Montgomery DC (1995) Response surface methodology: process and product optimization using designed experiments. Wiley, New York
44. Langhaar HL (1957) Dimensional analysis and theory of models. Wiley, New York
45. Gadalla AM, Tsai W (1989) Machining of WC-Co composites. Adv Mater Manuf Process 4(3):411–423
46. Gadalla AM, Tsai W (1989) Electrical discharge machining of tungsten carbide-cobalt composites. J Am Ceram Soc 72(8):1396–1401
47. Patil NG, Brahmankar PK (2008) Some investigations into surface characteristics of wire electro-discharge machined metal matrix composites. Proceedings of the 2nd International & 23rd All India Manufacturing Technology, Design and Research Conference, pp 747–752
48. Perez R, Carron J, Rappaz M, Walder G, Rewaz B, Flukiger R (2007) Measurement and metallurgical modelling of the thermal impact of EDM discharges on steel. Proceedings of the 15th International Conference on Electromachining, ISEM-XV: 17–22